Electronic Supporting Information

Small-molecule semiconductors containing dithienylacrylonitrile for high-performance organic field-effect transistors

Dizao Li,[a] Jiabin Zou,[ab] Congyuan Wei,[ac] Yankai Zhou,[ab] Liping Wang,[*b] Weifeng Zhang[a] and Gui Yu[*ac]

[a] Beijing National Laboratory for Molecular Sciences, CAS Research/Education Center for Excellence in Molecular Sciences, Institute of Chemistry, Chinese Academy of Sciences, Beijing 100190, P. R. China

[b] School of Materials Science and Engineering, University of Science and Technology Beijing, Beijing 100083, P. R. China

[c] School of Chemical Sciences, University of Chinese Academy of Sciences, Beijing 100049, P. R. China

1. **Device fabrications and performances of the organic field-effect transistors (OFETs).**

The OFET devices based on the small-molecular compounds were fabricated with bottom gate bottom contact (BGBC) configurations. The n^{++}-Si/SiO$_2$ (300 nm) substrates were used as the gate electrode/dielectric. The gold/titanium (30 nm/5 nm) was fabricated as source/drain electrodes. The silica substrates were modified with octadecyltrichlorosilane (OTS) to form an OTS self-assembled monolayer on their surfaces. A small-molecule semiconducting thin film layer was fabricated on the OTS-treated substrate by spin-coating. The device performance was evaluated by employed a Keithley 4200 SCS semiconductor parameter analyzer on a probe stage in ambient air. The charge carrier mobility (μ) was calculated from the data in the saturated regime according to the following equation,

$$I_{DS} = (\frac{W}{2L})C_i\mu(V_G-V_T)^2$$

In the above equation, I_{DS}, W/L, C_i, V_G and V_T are the saturation drain current, the channel width/length, the capacitance per unit area of the gate dielectric layer, the gate voltage and threshold voltage, respectively.

2. TGA curves of the DPP-DTE-based compounds
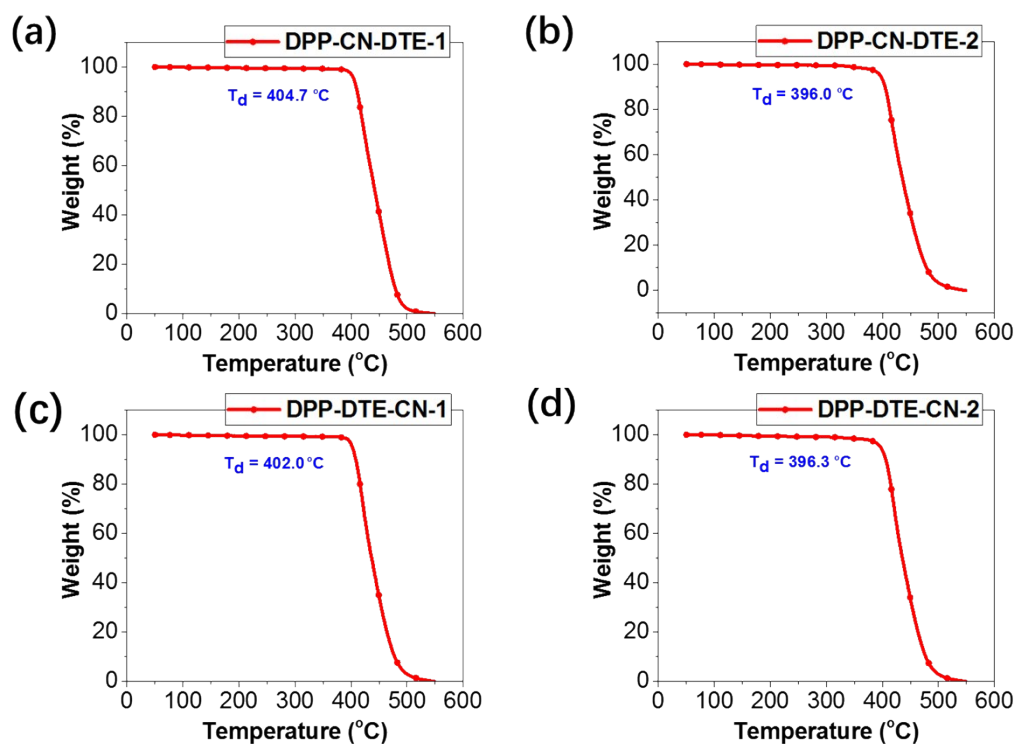
Fig. S1 TGA curves of the DPP-DTE-based compounds.

3. Absorption spectra of the DPP-DTE-based compounds
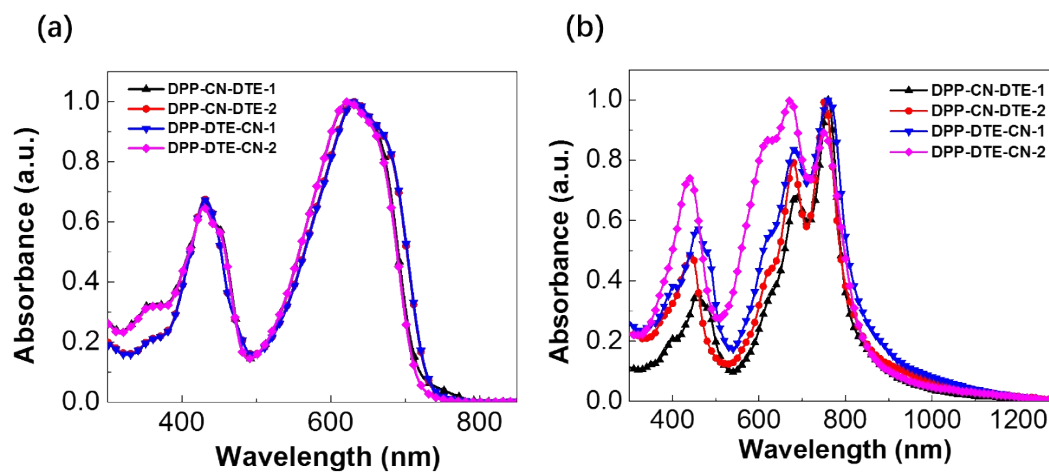
Fig. S2 UV-Vis-NIR absorption spectra of the DPP-DTE-based compounds in (a) chloroform solutions and (b) thin films.

4. Theoretical calculation results of the DPP-DTE-based compounds
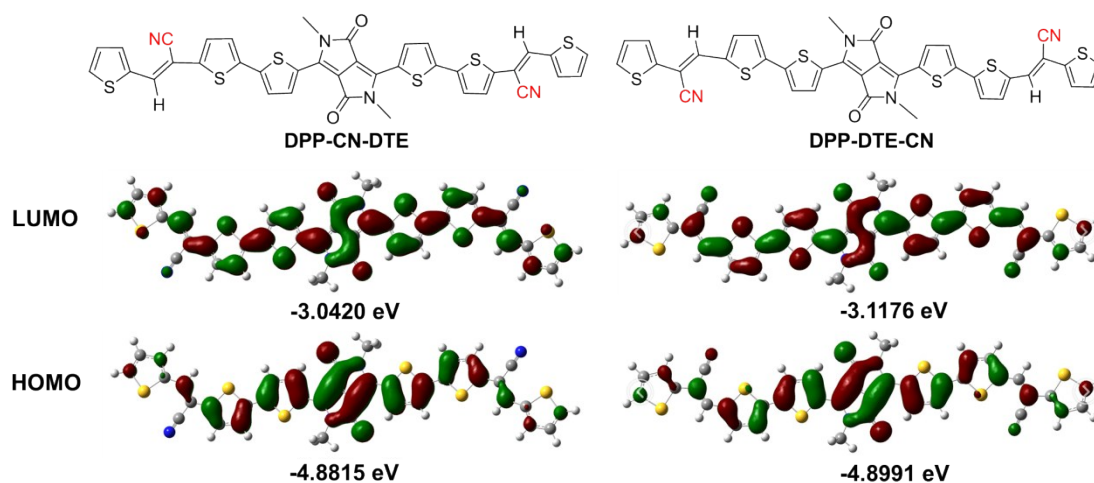
Fig. S3 Optimized molecular geometries and frontier molecular orbital distributions of the model compounds DPP-CN-DTE and DPP-DTE-CN.

5. NMR spectra of the DPP-DTE-based compounds
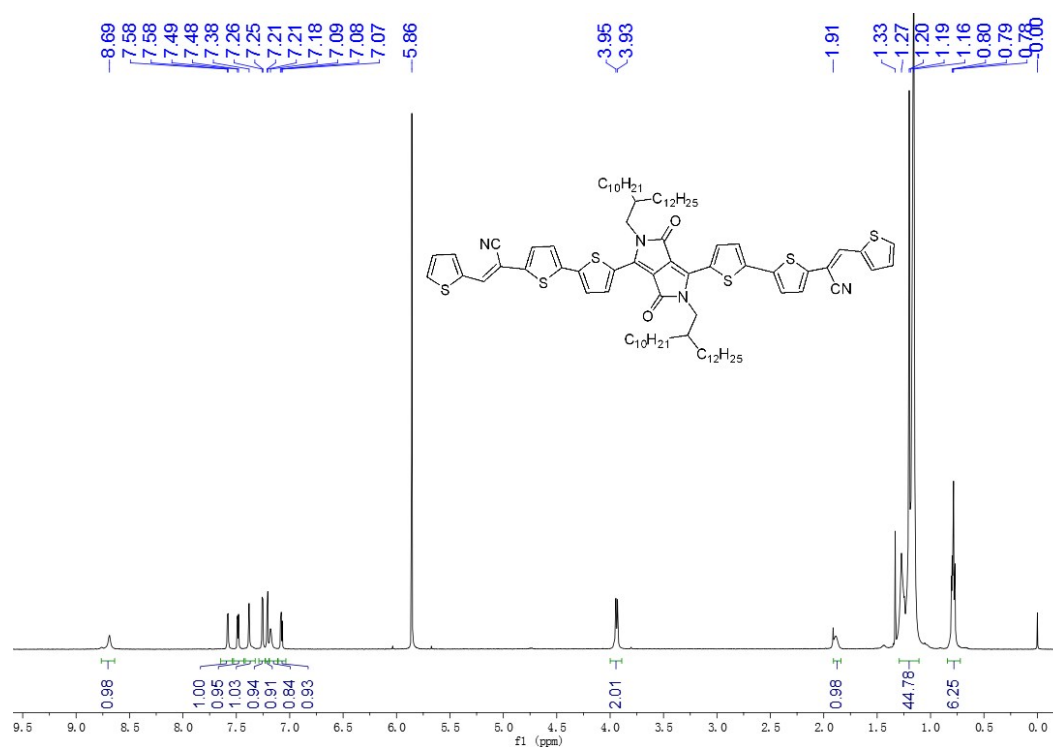
Fig. S4 ^{1}H NMR spectrum of DPP-CN-DTE-1.
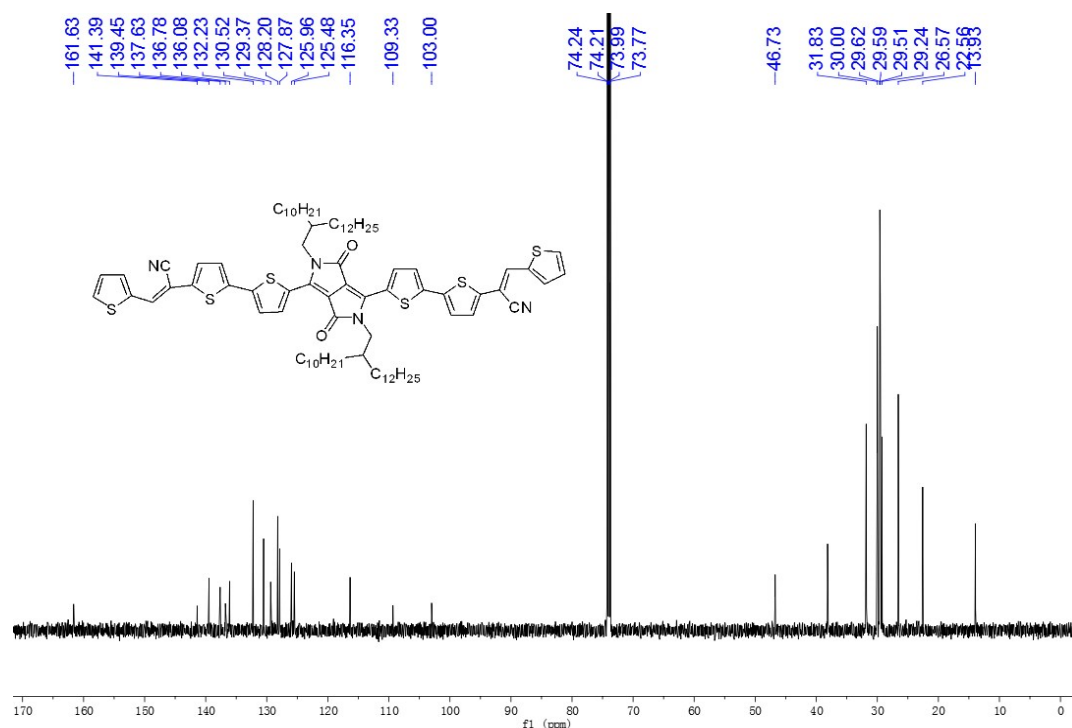
Fig. S5 ^{13}C NMR spectrum of DPP-CN-DTE-1.
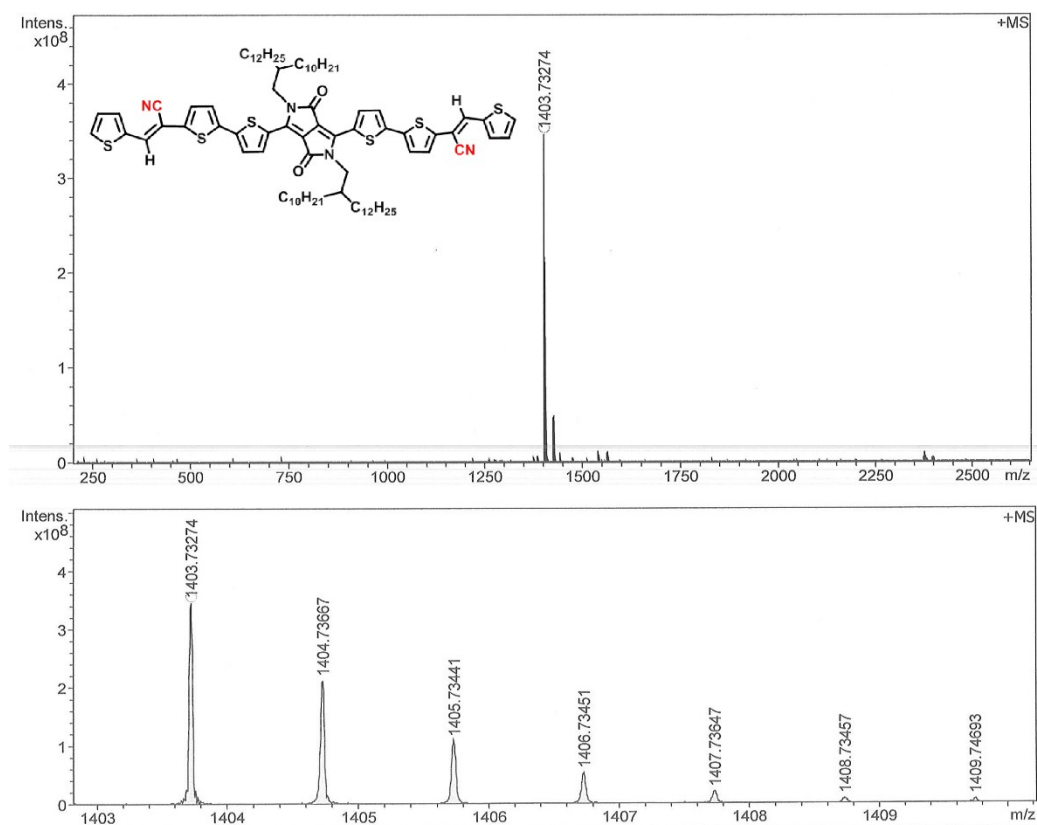
Fig. S6 HRMS (MALDI) spectrum of DPP-CN-DTE-1.
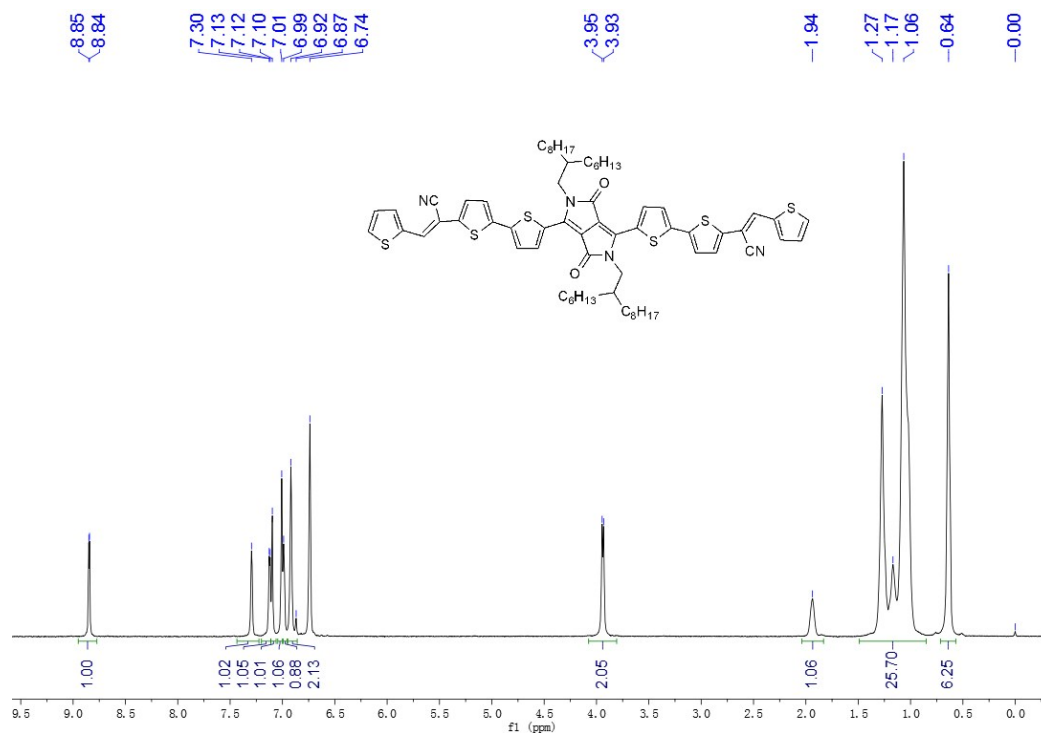
Fig. S7 ^{1}H NMR spectrum of DPP-CN-DTE-2.
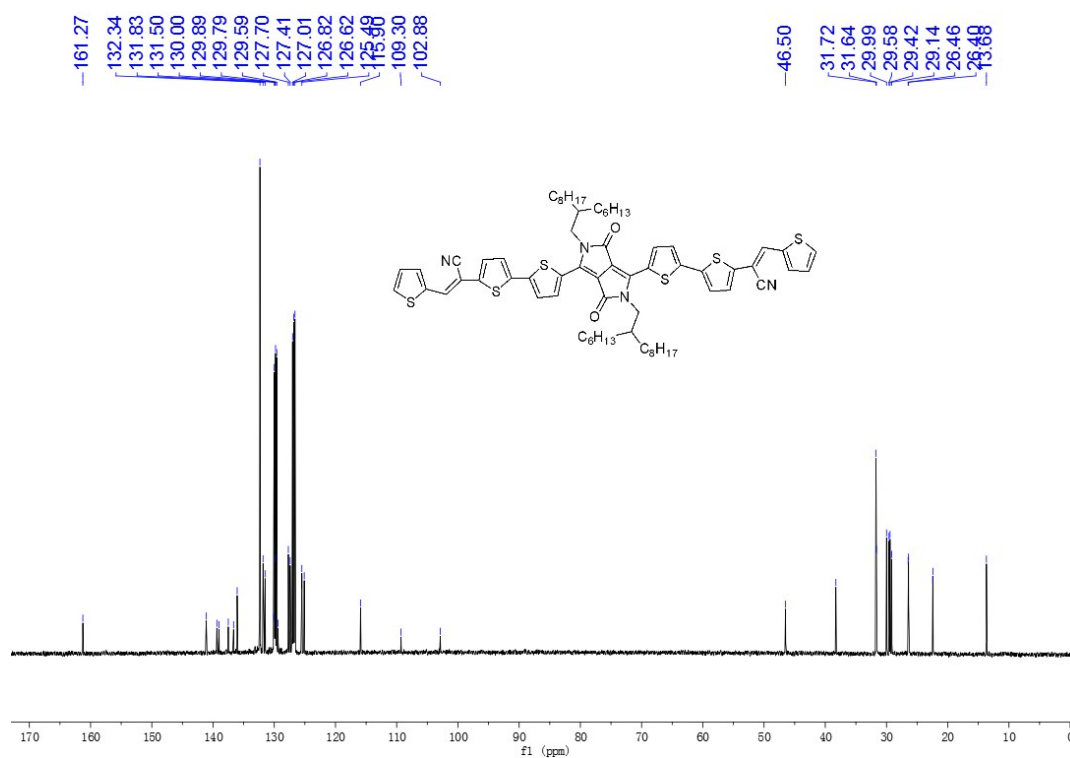
Fig. S8 ^{13}C NMR spectrum of DPP-CN-DTE-2.
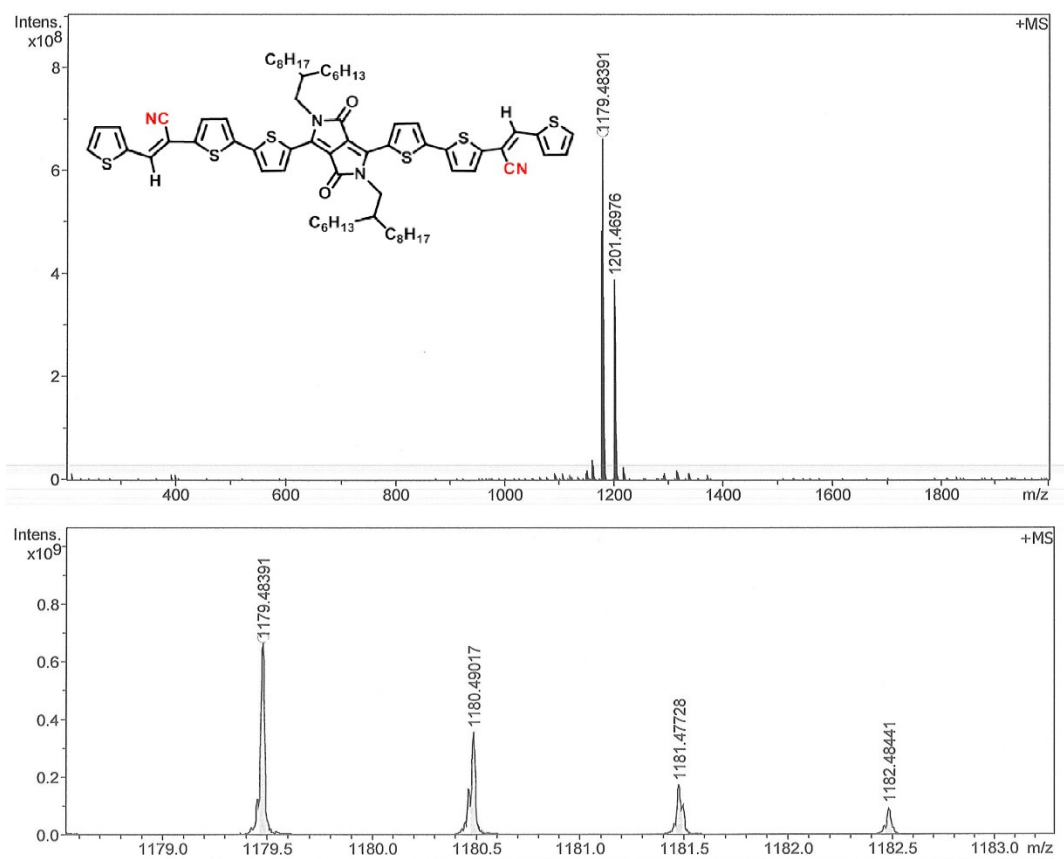
Fig. S9 HRMS (MALDI) spectrum of DPP-CN-DTE-2.
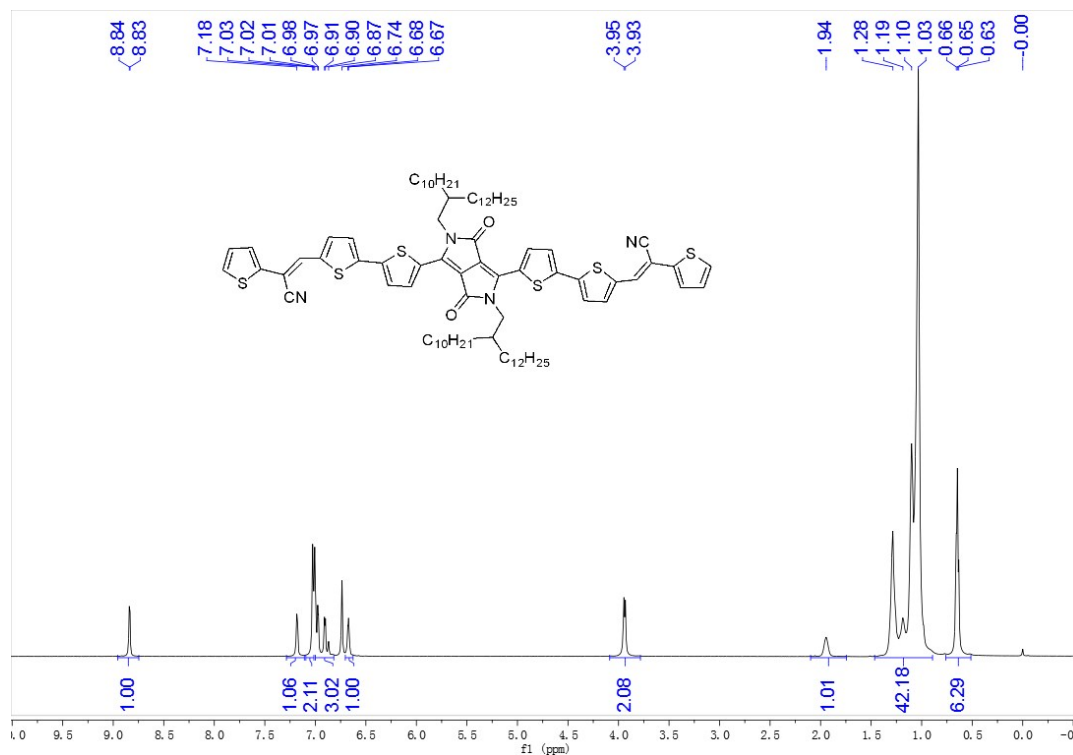
Fig. S10 ^{1}H NMR spectrum of DPP-DTE-CN-1.
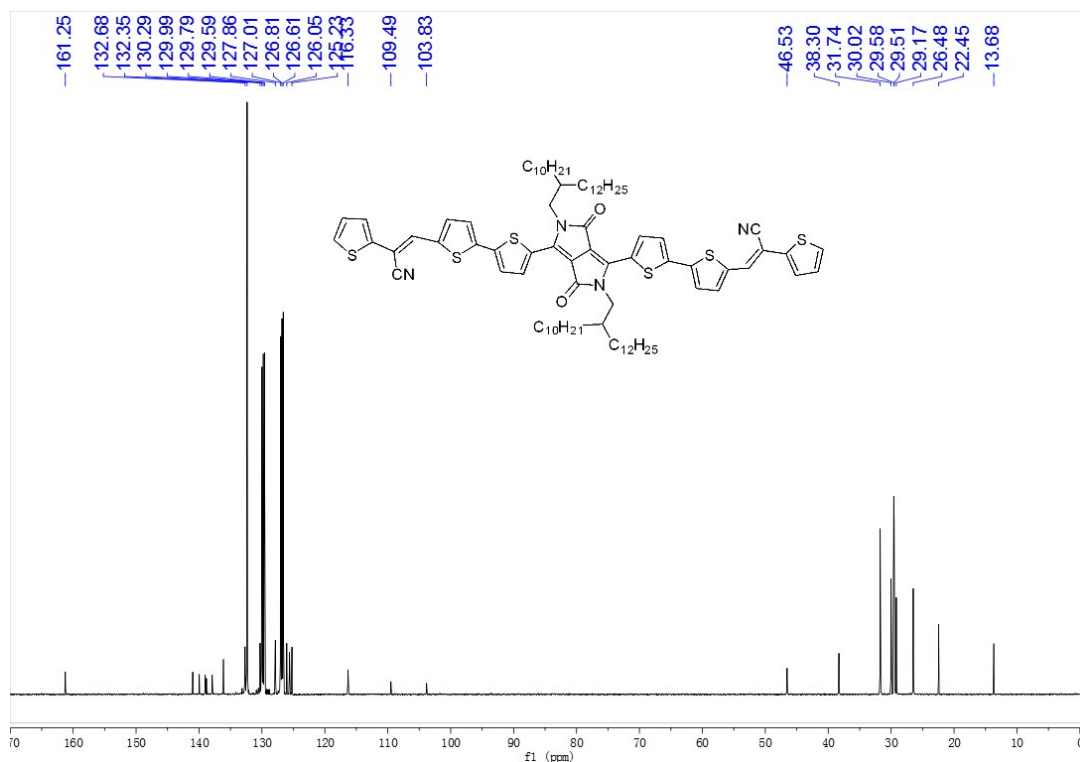
Fig. S11 ^{13}C NMR spectrum of DPP-DTE-CN-1.
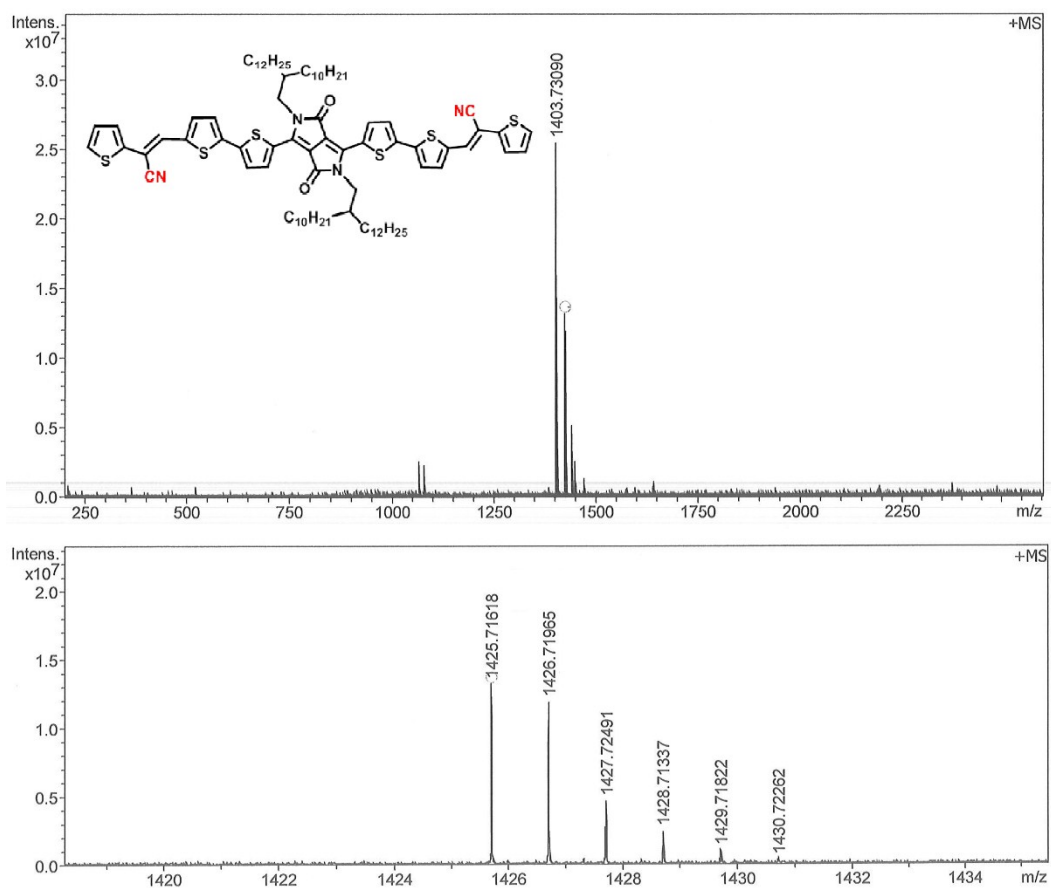
Fig. S12 HRMS (MALDI) spectrum of DPP-DTE-CN-1.
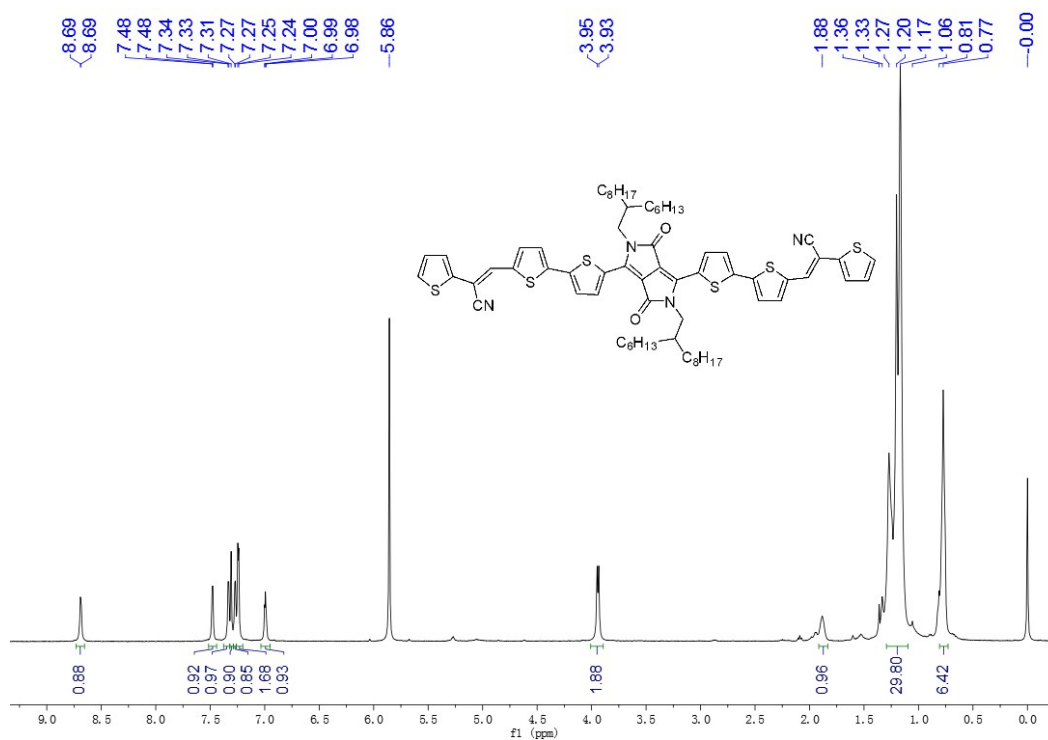
Fig. S13 ^{1}H NMR spectrum of DPP-DTE-CN-2.
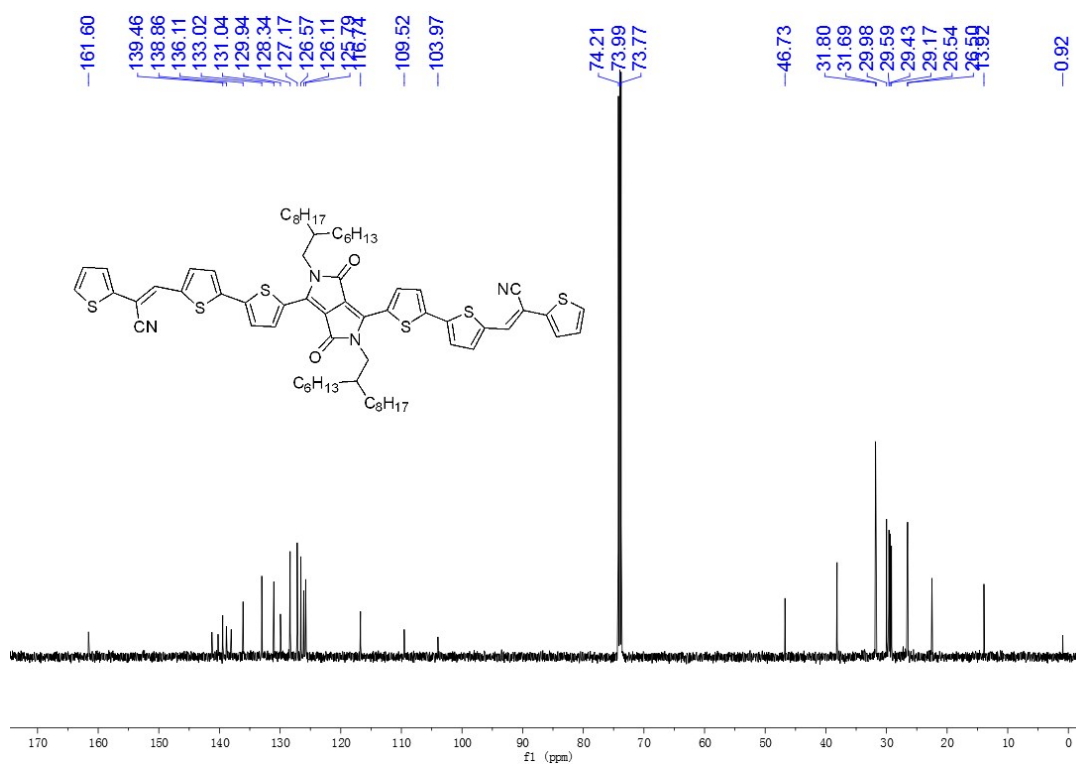
Fig. S14 ^{13}C NMR spectrum of DPP-DTE-CN-2.
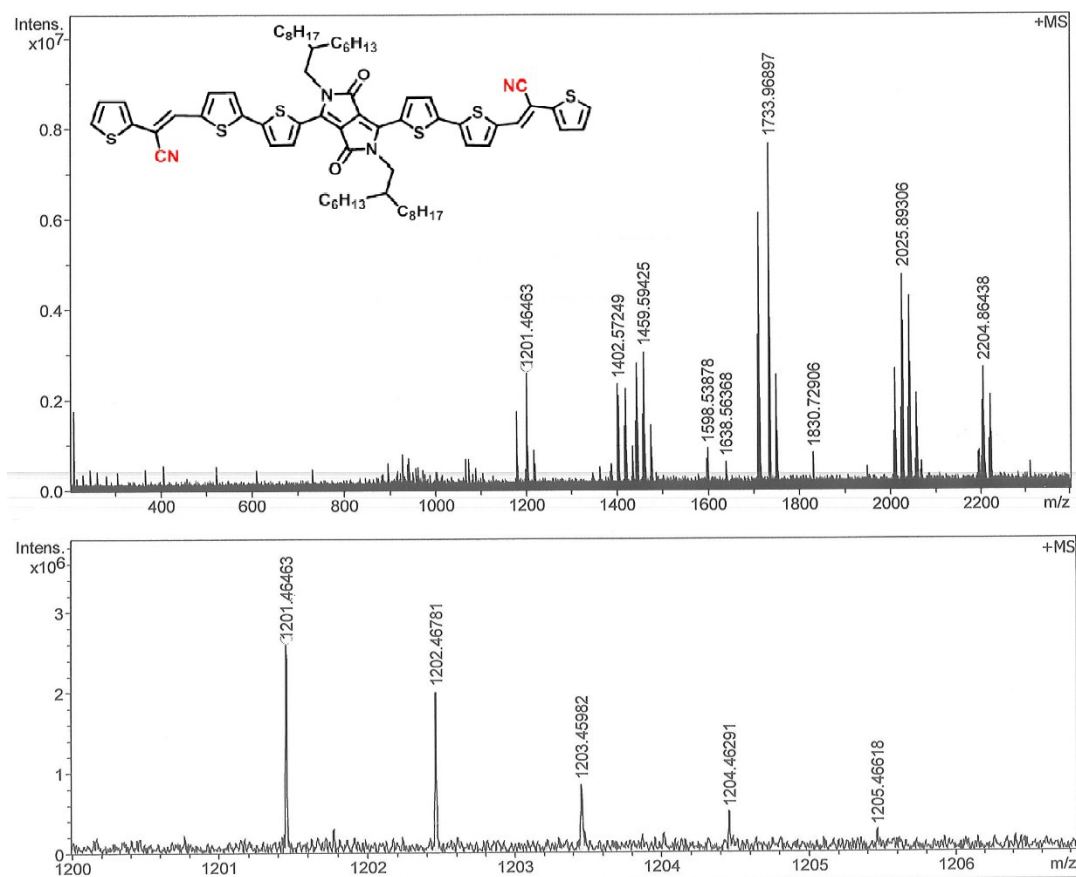
Fig. S15 HRMS (MALDI) spectrum of DPP-DTE-CN-2.